Journal of Materials Chemistry

www.rsc.org/materials

Volume 19 | Number 37 | 7 October 2009 | Pages 6625–6916

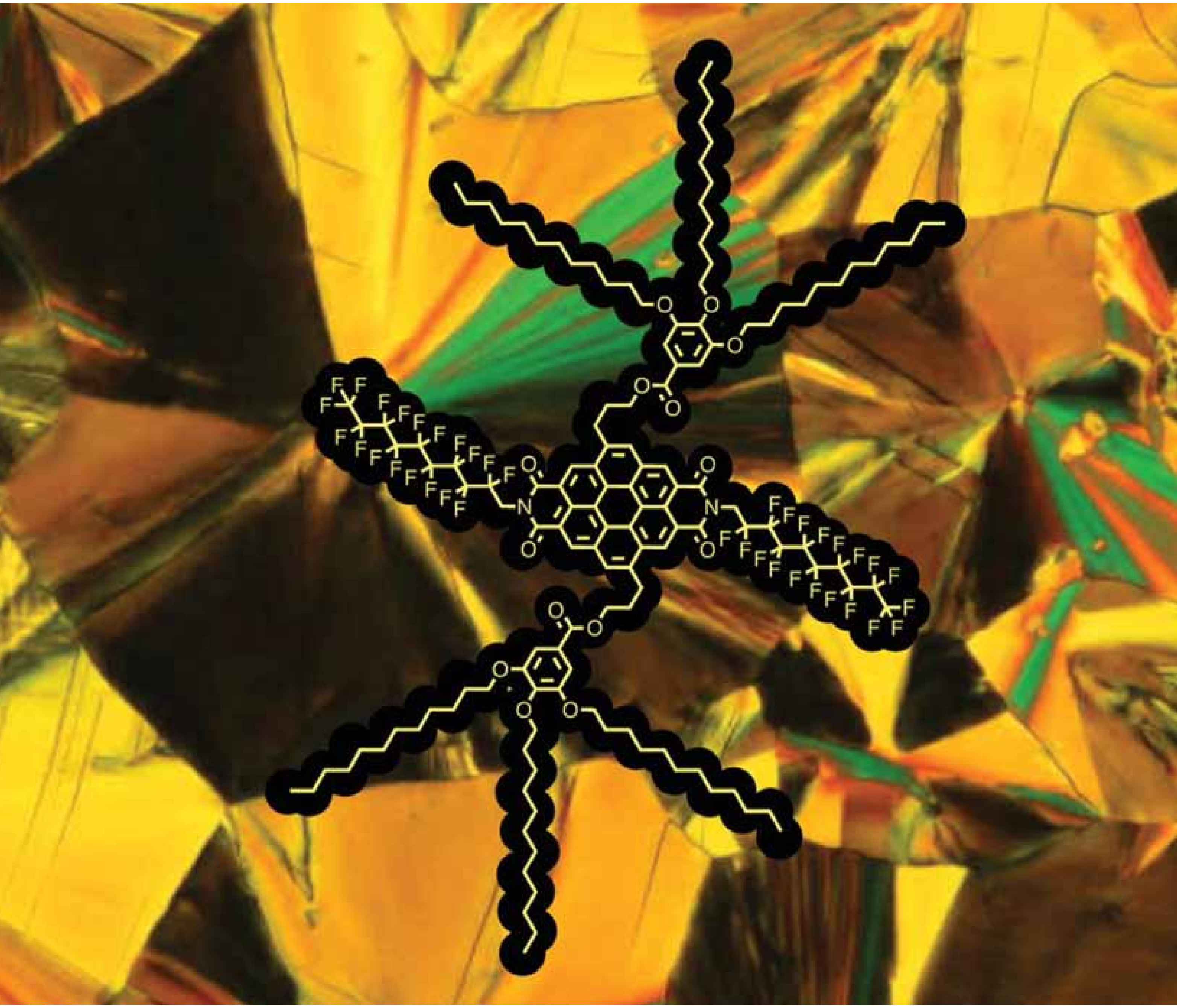

ISSN 0959-9428

RSC Publishing

PAPER
Seth R. Marder *et al.*
Room-temperature discotic liquid-crystalline coronene diimides exhibiting high charge-carrier mobility in air

FEATURE ARTICLE
Uday Maitra *et al.*
Supramolecular gels 'in action'

0959-9428(2009)19:37;1-M

Room-temperature discotic liquid-crystalline coronene diimides exhibiting high charge-carrier mobility in air†

Zesheng An,[a] Junsheng Yu,[b] Benoit Domercq,[b] Simon C. Jones,[a] Stephen Barlow,[a] Bernard Kippelen*[b] and Seth R. Marder*[a]

Received 3rd June 2009, Accepted 17th July 2009
First published as an Advance Article on the web 18th August 2009
DOI: 10.1039/b910898j

Six *N*,*N*′,5,11-tetrasubstituted coronene-2,3,8,9-tetracarboxydiimides have been synthesised incorporating 3,4,5-tri(*n*-dodecyloxy)phenyl or 2-(*n*-decyl)-*n*-tetradecyl groups in various positions. Differential scanning calorimetry, polarised optical microscopy, and X-ray diffraction indicate that all form columnar discotic mesophases from around room temperature to around 200 °C. Charge-carrier mobility values, which energetic considerations suggest are electron mobility values, have been determined in non-aligned samples cooled from the isotropic melt using the space-charge-limited current technique. The highest mobility, 6.7 $cm^2\ V^{-1}\ s^{-1}$, was found in *N*,*N*′-bis(*n*-2,2,3,3,4,4,5,5,6,6,7,7,8,8,8-pentadecylfluorooctyl)-5,11-bis(3-[{3,4,5-tri(*n*-dodecyloxy)phenyl}carbonyloxy]-*n*-propyl)coronene-2,3,8,9-tetracarboxydiimide, which X-ray diffraction suggests is the most highly ordered of the materials examined.

Introduction

Compounds that form columnar discotic liquid-crystalline (LC) mesophases have attracted attention as possible hole- and electron-transport materials for applications in organic electronic devices.[1] These materials offer the possibility for high degrees of order and extensive π-orbital overlap leading to high intrachain charge-carrier mobilities, while potentially being more readily processed from solution or from an isotropic melt than π-stacked single-crystal materials, and are typically composed of molecules in which a central planar redox-active π-delocalised core is surrounded by flexible side chains.[2] Therefore, extensive efforts have been directed towards developing and studying columnar discotic materials as hole- and electron-transport materials;[3–15] a few examples have been reported with charge-carrier mobility values in the columnar phase exceeding 1 $cm^2\ V^{-1}\ s^{-1}$.[16–18]

Perylene-3,4:9,10-tetracarboxydiimides, **I** (Fig. 1), have attracted interest as electron-transport materials;[19–30] very high electron mobility values of 1.7 and 1.3 $cm^2\ V^{-1}\ s^{-1}$ have been obtained from field-effect measurements on polycrystalline films of **Ia**[31] and from space-charge-limited current (SCLC) measurements on a columnar LC mesophase of **Ib**,[18] respectively. The related coronene-2,3:8,9-tetracarboxydiimides appear to be interesting candidates for transport materials; while there is not a universal correlation between core size and mobility,[17] it has been reported that for some series of compounds increased core sizes lead to stronger intermolecular interactions and, hence, to increased charge-carrier mobility.[32] However, although coronene diimides and related systems have been the subject of a number of studies,[33–42] there is little information available regarding charge mobility in these materials. Indeed, to the best of our knowledge, the only report of a charge-carrier in a coronene imide derivative is for a 2,3-dicarboxymonoimide derivative, **III** (Fig. 1), for which a 1D intrastack carrier mobility as high as *ca.* 0.3 $cm^2\ V^{-1}\ s^{-1}$ was obtained using the PR-TRMC technique.[34] Columnar coronene diimides previously reported by Rohr *et al.*,[33,34] **IIa** (Fig. 1), were found to form mesophases only at rather high temperatures (>177 °C) at which mobility measurements were deemed impractical. No mobility data have been reported for an example with long "swallow-tail" *N*,*N*′-substituents, **IIb** (that forms a columnar phase, assigned to a plastic crystalline phase) at temperatures between room temperature and 285 °C.[39] Here, we report the synthesis and characterisation of six 6,11,*N*,*N*′-substituted coronene-2,3:8,9-tetracarboxydiimides, **1a–c**, **2** and **3** (Scheme 1), in which 3,4,5-tris(*n*-dodecyloxy)phenyl groups are linked to either *N*,*N*′ (**1a–c**) or 6,11 (**2**) positions, or in which long branched alkyl groups are attached to the *N*,*N*′ positions, with the aim of lowering the phase-transition temperatures. We describe the synthesis of these compounds, following the procedure previously reported by Rohr *et al.*;[33,34] characterisation of their mesophase behaviour using optical polarised microscopy (OPM), differential scanning calorimetry (DSC) and X-ray diffraction (XRD); and measurements of charge-carrier mobility using the SCLC technique.

Results and discussion

Synthesis

As noted above, a series of *N*,*N*′,5,11-tetrasubstituted coronene-2,3,8,9-tetracarboxydiimides, **IIa**, have previously been synthesised

---

[a] *School of Chemistry and Biochemistry and Center for Organic Photonics and Electronics, Georgia Institute of Technology, Atlanta, Georgia, 30332, USA. E-mail: seth.marder@chemistry.gatech.edu*

[b] *School of Electrical and Computer Engineering and Center for Organic Photonics and Electronics, Georgia Institute of Technology, Atlanta, Georgia, 30332, USA. E-mail: kippelen@ece.gatech.edu*

† Electronic supplementary information (ESI) available: NMR spectra showing isomer mixture present for **3**; UV-vis absorption and emission data; UV-vis data showing aggregation; examples of cyclic voltammograms; polarised optical microscopy images; X-ray diffraction patterns and indexing for all 6 compounds; diffraction pattern for **2b** at 100 °C. See DOI: 10.1039/b910898j

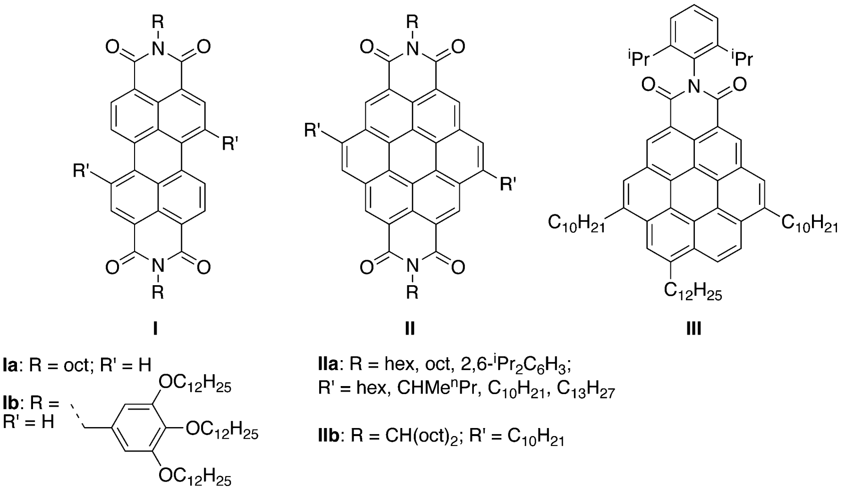

Fig. 1 Structures of perylene diimide, **I**, coronene diimide, **II**, and a coronene monoimide, **III**, discussed in the text.

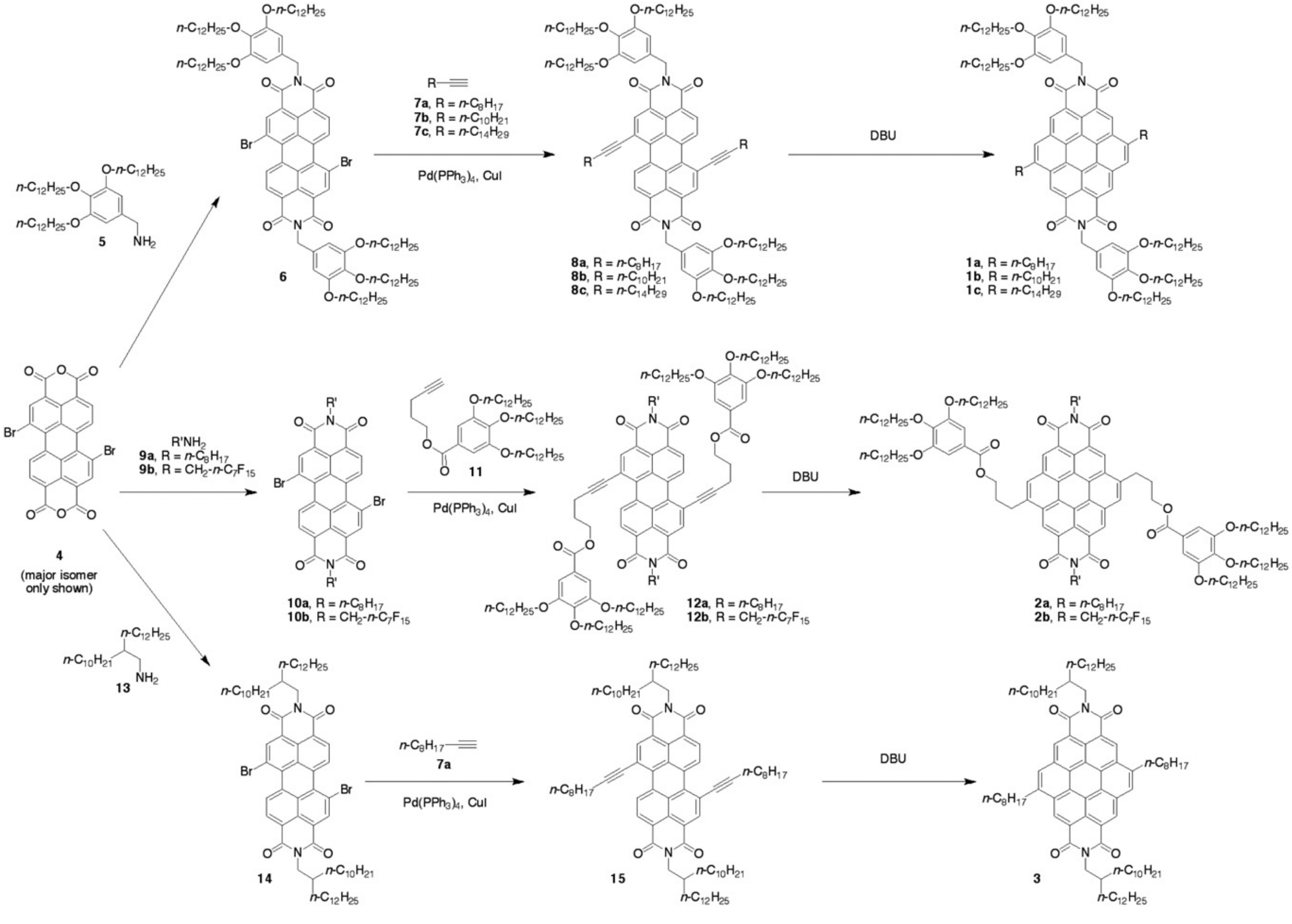

Scheme 1

by Rohr *et al.* and found to exhibit LC behaviour only at high temperatures.[34] The substituents used were generally straight chain alkyl groups (with short branched substituents being used in the 5,11 positions of one example and 2,6-di(isopropyl)phenyl groups being used as *N*,*N*′ substituents in another). In the hope of lowering the LC transition temperatures, we chose to investigate the use of 3,4,5-tris(*n*-dodecyloxy)benzyl groups, attached either directly in the *N*,*N*′ positions (**1a–c**) or through long linkers to the 5,11 positions (**2a,b**), or the long "swallow-tail" 2-(*n*-decyl)-*n*-tetradecyl groups in the *N*,*N*′ positions (**3**). Indeed a similar long-chain branched substituent in the *N*,*N*′ position to that in **3** was used by Nolde and co-workers to obtain a coronene diimide, **IIb**, with a markedly lower isotropic melting point.[39] Scheme 1 shows the syntheses of the six coronene diimides discussed here, which are closely analogous to those of the coronene diimides reported by Rohr *et al.*[34] Thus, 1,7-dibromoperylene-3,4:9,10-tetracarboxyanhydride, **4**,[43] is first converted to a 1,7-dibromoperylene-3,4:9,10-tetracarboxydiimide (**6**, **10a,b**, or **14**) using the appropriate amine (**5**,[44] the commercially available **9a,b**, or **13**[45]), which is then coupled with the appropriate terminal alkyne (the commercially available species **7a–c** or the new compound **11**) under Sonogashira conditions.[46] The resulting 1,7-dialkynyl perylene diimide derivatives (**8a–c**, **12a,b**, **15**) are then cyclised to give the coronene diimides using diazabicyclo[5.4.0]undec-7-ene (DBU). In some cases, the intermediate dialkynyl species were not isolated, but were converted *in situ* to the coronene diimides by addition of DBU to the reaction mixture. In the case of **2b**, some cyclisation of **12b** to the final product was observed even prior to the addition of DBU.

It should be noted that bromination of perylene-3,4:9,10-tetracarboxydianhydride in concentrated sulfuric acid can give 1,6,7-tribromo and 1,6-dibromo derivatives in addition to the 1,7-dibromo compound, **4**,[47] with the isomer ratio depending somewhat on the reaction conditions (we find that, generally, the use of more bromine, higher temperature, or longer reaction time tends to lead to formation of more of the 1,6 isomer). While any tribrominated species are easily removed from soluble diimides derived from the brominated dianhydride by column chromatography, separation of the 1,6 and 1,7 isomers is less straightforward. Therefore, formation of all of the 1,7-substituted perylene and 5,11-substituted coronene derivatives shown in scheme 1 is accompanied by formation of small amounts of the 1,6- and 5,12-substituted derivatives, respectively. Thus, as in previous work on LC coronene diimides,[34] subsequent characterisation was performed using isomer mixtures. While Rohr *et al.* obtained a 96 : 4 isomer ratio, we found an 88 : 12 ratio from a 500 MHz ^{1}H NMR study of **3** (see ESI† for details).

Optical and electrochemical properties

The UV-vis absorption spectra of coronene diimides **1a–c**, **2a,b** and **3** in dilute dichloromethane solution (see ESI†) are essentially identical to one another and to those previously reported for other coronene diimides.[33,34,38] The compounds are weakly fluorescent in dichloromethane; the spectra (see ESI†) closely resemble to those previously reported for annealed dilute dispersions of coronene diimides in polystyrene.[33] Although one might naively anticipate that extension of the π-system from perylene to coronene diimide would lead to a red shift in the absorption, in fact a blue shift is observed and also predicted by quantum-chemical calculations.[35] In methylcyclohexane, a much less polar solvent, there is evidence for significant aggregation, with solutions of concentrations of *ca.* 10^{-5} M closely resembling those of drop-cast films. Variable concentration studies for **1a–c** and **3** (see ESI†) suggest aggregation constants in the range $0.8–5.1 \times 10^5$ M^{-1}, increasing in the order **3** < **1a** < **1c** < **1b**. These values suggest significant intermolecular interactions and fall within the range of aggregation constants estimated in the same way for perylene diimide discotic mesogens; values of 1.3×10^4 and *ca.* 10^7 M^{-1} have been reported for *N*,*N*′-bis[3,4,5-tri(*n*-dodecyloxy)benzyl] and *N*,*N*′-bis[3,4,5-tri(*n*-dodecyloxy)phenyl] derivatives, respectively.[48]

Perylene diimides typically exhibit two electrochemically reversible molecular reductions; for example, we have previously noted that **Ib** is successively reduced at −1.02 and −1.21 V *vs.* ferrocenium/ferrocene in dichloromethane–0.1 M ^{n}Bu$_4$NPF$_6$.[18] Under the same conditions the present coronene diimides exhibit less straightforward molecular reduction features in their voltammograms; these are not electrochemically reversible (see ESI†), perhaps in part due to complications related to aggregation. This hampers direct comparison with perylene diimides. However, the first reduction potential appears to be *ca.* −1.4 V *vs.* ferrocenium/ferrocene for **1a–c**, **2a**, and **3**, suggesting the LUMO for these species to be some 0.4 eV higher in energy than that of perylene diimides (*i.e.* the EA for these species is *ca.* 3.7 eV using a value of 4.1 eV for perylene diimides[18,49]), consistent with quantum-chemical calculations which predict that the LUMO and HOMO of coronene diimides are higher and lower, respectively, in energy than those of perylene diimides.[35] No molecular oxidation is detected in the accessible potential range, but the IP can be estimated from the estimated EA and the optical gap (obtained from intersection of normalised absorption and fluorescence spectra as 2.4 eV) to be in excess of 6.1 eV (this estimate neglects the exciton binding energy and so represents a lower limit). Compound **2b** appears to be somewhat more easily reduced than the other coronene diimides with a potential of *ca.* −1.1 eV, suggesting that HOMO and LUMO both lie *ca.* 0.3 eV lower in this system. This effect is presumably due to the inductive electron-withdrawing properties of the $CH_2C_7F_{15}$ substituents. Similar effects on the electrochemical properties of naphthalene and perylene diimides have previously been observed upon partial fluorination of the *N*-alkyl groups.[26,27,50]

Thermal properties and mesophase structure

A differential scanning calorimetry (DSC) trace for **2b** is shown as an example in Fig. 2; all six compounds show qualitatively similar behaviour, with a transition at room temperature or lower and an isotropic clearing point at *ca.* 180–250 °C (Table 1). Optical polarised microscopy and X-ray diffraction (discussed below) are consistent with assignment of the phases stable

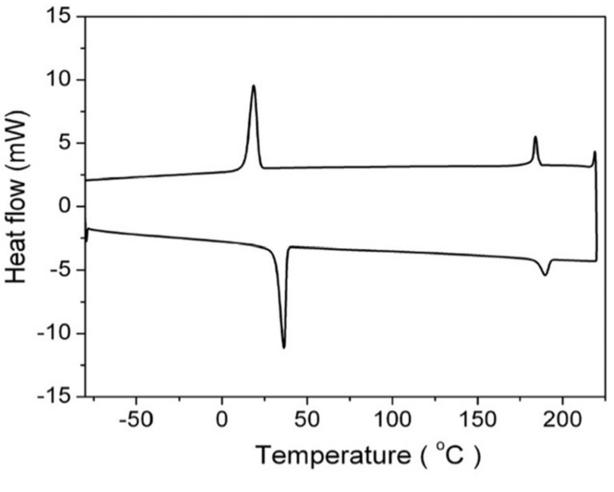

Fig. 2 Differential scanning calorimetry trace (10 °C min^{-1}, second heating–cooling cycle) for **2b**.

Table 1 Transition temperatures (°C) with enthalpy changes (kJ mol^{-1}) in parentheses for coronene diimides measured by DSC (10 °C min^{-1})[a]

	2nd heating		2nd cooling	
Compound	Cr → Col	Col → I	I → Col	Col → Cr
1a	27 (17)	188 (9.6)	179 (7.8)	0 (51)
1b	16 (48)	182 (11)	175 (11)	9 (43)
1c	19 (62)	181 (12)	174 (12)	11 (69)
2a	28 (20)	205 (6.8)	201 (6.4)	11 (21)
2b	36 (67)	189 (13)	184 (13)	19 (64)
3	−13 (3.6)	254 (5.9)	250 (5.9)	−26 (7.2)

[a] Cr, Col, and I denote phases assigned to crystal, columnar discotic liquid crystal, and isotropic liquid, respectively.

between *ca.* room temperature and *ca.* 200 °C as columnar discotic LC phases. The low temperature transition is, therefore, likely to be a Cr → Col transition, where Cr and Col denote crystalline and columnar discotic LC phases, respectively, although we cannot rule out the possibility that the lowest temperature phase is in fact another LC phase. These transition temperatures are considerably lower than those reported for a range of *N*,*N*′,5,11-tetraalkyl coronene diimides **IIa** (the lowest Cr → Col transition in the series was observed at 177 °C),[34] and a little lower than for **IIb** (Cr → Col < 20 °C; Col → I at 285 °C, where I denotes the isotropic phase).[39]

Polarised optical microscopy for films of all six compounds obtained from cooling from the isotropic melt to room temperature shows textures consistent with the presence of columnar order. Micrographs **1a** and **2b** are shown in Fig. 3; data for the other compounds are shown in the ESI†. X-Ray diffraction (XRD) confirms the presence of columnar order in all cases; with the exception of **1b**, for which the reflections can be indexed to a rectangular cell, the diffraction patterns can all be indexed to hexagonal cells (see ESI† for indexing of diffraction patterns). For **1a** (Fig. 1a), only two diffraction peaks, attributed to the (100) and (110) reflections of a hexagonal cell, are observed in the low-angle region. However, **1c**, which has longer side chains attached to the coronene core, displays four diffraction peaks from (100) to (210), suggesting a higher degree of molecular ordering than in the mesophase of **1a**. Films of **2b** show considerably more diffraction peaks than **2a** and the crystal-to-mesophase transition occurs at higher temperature for the former compound, suggesting that the perfluoroalkyl group significantly enhances the ordering of room temperature films, perhaps through improved alignment of the molecules by fluorophobic interaction between the fluoroalkyl group and the hydrocarbon moieties. In all cases except **2b**, a very broad "alkyl halo" is observed centred at a diffraction angle of *ca.* 20°. In **2b**, the broad halo is seen at a slightly lower value of 2θ (*ca.* 17–18°), consistent with assignment to the fluoroalkyl chains,[51] while a relatively sharp feature within the "alkyl halo" region (2θ = *ca.* 21°) is perhaps indicative of increased ordering of the alkyl side chains at room temperature; on heating this peak is replaced by a broad feature at *ca.* 20°, overlapping with the fluoroalkyl halo, suggesting melting of the alkyl chains similar to that seen in the other compounds (see ESI† for an X-ray pattern at 100 °C). The X-ray patterns of most of the films, including those of **1a** and **2b** shown in Fig. 3, also exhibit a reasonably well-defined feature at *ca.* 25°, attributable to the separation between neighbouring aromatic cores along the column stacking direction; the distance of *ca.* 3.5° is similar to that seen for other columnar mesophases, such as those based on hexabenzocoronene[52,53] and that formed by the coronene diimide **IIb**,[39] and indicates the possibility of strong π–π overlap.

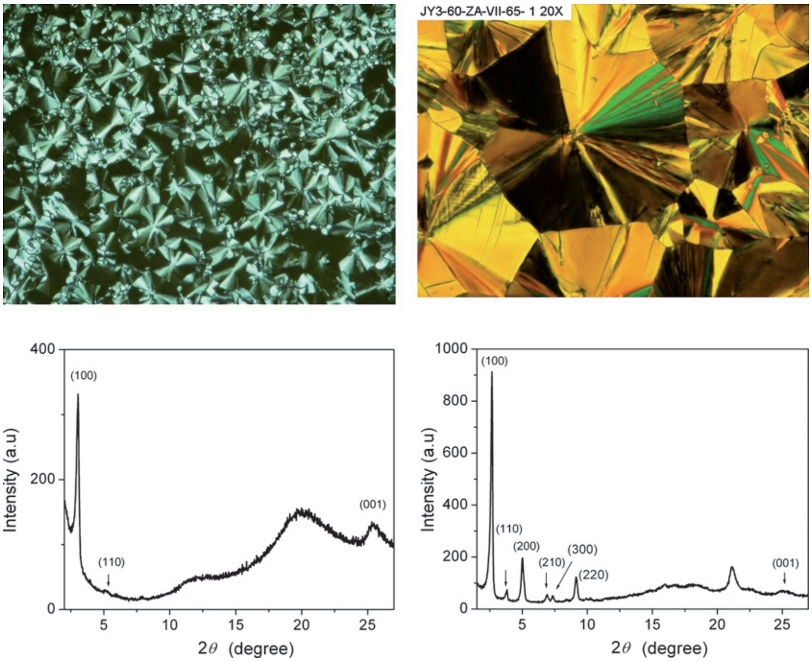

Fig. 3 Polarised optical microscopy images (top, image sizes are 615 × 460 μm in both cases) and room-temperature X-ray diffraction patterns (below) for **1a** (left) and **2b** (right).

SCLC carrier mobilities

The charge-carrier mobility in **1a–c**, **2a,b**, and **3** was investigated using the steady-state space-charge-limited current (SCLC) technique, which has been widely used to investigate carrier mobility in organic materials,[54–62] including several materials forming columnar discotic mesophases.[14,18,63,64] This technique uses the current–voltage characteristics of organic thin films sandwiched between injecting electrodes. The current typically exhibits a linear dependence on the voltage at low voltages and depends on two unknowns, the carrier density and carrier mobility. However, at high voltages, an approximately quadratic SCLC regime can be observed with appropriate combinations of sample geometry and electrode material; in this regime, if the contacts are assumed to be ohmic and the materials to be trap-free, the current depends only on the carrier mobility, μ, and on the capacitance of the sample, which can be measured independently. SCLC values of μ obtained neglecting the possibility of imperfectly ohmic injection can vary depending on the work function of the injecting electrodes and are, in general, similar to or lower than values obtained for the same material from (injectionless) time-of-flight measurements.[14,64–68]

Current density–voltage (*J*–*V*) characteristics were measured under ambient conditions for devices with geometry (+) ITO–coronene diimide (5 μm)–Ag (−) prepared by melting the coronene diimides between glass-supported electrodes. Fig. 4 shows data acquired for **2b** and **3**; in these and all other cases, a linear, *i.e.*, ohmic, dependence of *J* on *V* is observed at low voltages, while at higher applied voltages there is a transition to a regime assigned to SCLC in which the dependence can be fitted as $J \propto V^x$ where x is in the range 2.0–2.6. Based on the estimated IP and EA of the coronene diimides, electron injection from Ag (which has a work function of 4.2 eV) into the material is anticipated to be more favourable than hole injection from ITO (4.5 eV); therefore, electron injection is likely to be the dominant process and the mobility values derived from these *J*–*V* data are most likely those for electrons.

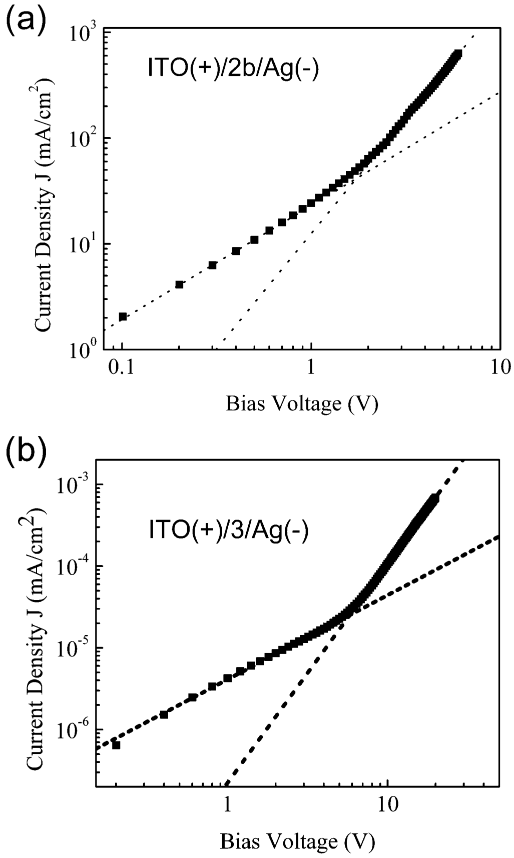

Fig. 4 *J*–*V* characteristics of coronene diimide (a) **2b** and (b) **3** in device geometry: (+) ITO–coronene diimide **2b** or **3** (5 μm)–Ag (−) under ambient conditions.

As in our previous work,[18,58,63,64] the approximately quadratic portions of the *J*–*V* curves were fitted to a modified Mott–Gurney equation:[69]

$$J = \frac{9}{8}\theta\varepsilon_0\varepsilon_r\mu_0 \exp\left(0.981\gamma\sqrt{\frac{V}{d}}\right)\frac{V^2}{d^3} \tag{1}$$

where $\theta \leq 1$ (deviating from unity when the injection is non-ohmic or the material contains charge-carrier traps), ε_0 is the permittivity of free space, ε_r is the relative dielectric constant of the transport material (obtained from capacitance measurements), μ_0 is the charge-carrier mobility in zero electric field, γ is a constant that is related to the field dependence of the mobility, and d is the sample thickness.

Values of μ_0 and γ obtained from the best fits of the *J*–*V* curves, assuming $\theta = 1$, are compared in Table 2, along with the maximum values of the mobility, μ_{max}, obtained from inserting these values and the maximum applied voltage into the equation:[70]

$$\mu_{max} = \mu_0 \exp\left(\gamma\sqrt{\frac{V}{d}}\right) \tag{2}$$

The values of mobility, which are discussed in more detail below, along with those of γ (which are typical values for organics), are collected in Table 2. Also in Table 2, we compare values of the threshold voltage, V_T, at which the *J*–*V* dependence changes from ohmic to SCLC obtained directly from the *J*–*V* plots, V_T(exp), and estimated the parameters used to fit the SCLC data to eqn (1), V_T(calcd). At V_T, the current density can be described using either Ohm's law or the Mott–Gurney expression; equating these two expressions leads to:

$$V_T = \frac{8}{9}en_{fb}\frac{d^2}{\varepsilon_0\varepsilon_r} \tag{3}$$

where e is the electronic charge and n_{fb} is the number of free background carriers in the ohmic regime, which can be estimated by extracting the carrier density for the linear regime using an estimate of the mobility derived from eqn (1) and (2). We note that the agreement between the experimental and calculated values of the threshold voltage is not perfect; however, both values remain within the same order of magnitude. Considering that both the density of free carriers and the carrier mobility can vary each by several orders of magnitude in materials tested with SCLC experiments, this result constitutes an important self-consistency test when performing these experiments.

With the exception of **3**, the new coronene diimides all show very high effective charge-carrier mobility. Moreover, as noted

Table 2 SCLC charge-carrier mobility values and associated parameters for coronene diimides

Compound	ε_r[a]	μ_0[b]/cm^2 V^{-1} s^{-1}	γ[b]/10^{-3} cm$^{0.5}$ V$^{-0.5}$	μ_{max}[c]/cm^2 V^{-1} s^{-1}	V_T(calcd)[d]/V	V_T(exp)[d]/V
1a	2.0	0.44	1.6	0.54 (at 7.5 V)	2.4	3
1b	2.7	1.78	4.3	3.0 (at 7.5 V)	1.1	3
1c	2.6	2.04	3.5	3.1 (at 7.5 V)	2.4	3
2a	2.8	4.3	0.81	4.7 (at 6.6 V)	3.9	3
2b	3.4	4.0	4.7	6.7 (at 6 V)	1.2	2
3	2.6	1.9×10^{-7}	9.0	1.1×10^{-6}	1.9	6

[a] Relative dielectric constant from capacitance measurements. [b] Determined by best fit of approximately quadratic portion of J–V curve to eqn (1), assuming $\theta = 1$. [c] Determined from eqn (2) and the maximum voltage applied. [d] V_T(calcd) and V_T(exp) are threshold voltages for SCLC transport and are estimated from equating Ohm's law and the Mott–Gurney expression, as described in the text, and determined from the intersection of linear fits to the ohmic and SCLC regions in a log J–log V plot, respectively.

above, these mobility values were obtained by assuming ohmic injection and trap-free transport ($\theta = 1$) and, therefore, represent lower limits for the mobility in these samples. Indeed, the effective mobility values for some of these species exceed those that we have observed using the same technique in the columnar discotic perylene diimide **1b**,[18] perhaps due to the increased core size of the coronene compounds leading to more effective intermolecular interactions, and are among the highest measured for molecular materials.

Several factors limit the extent to which structure–property relationships within the series of coronene diimides examined can be made. Firstly, it should be noted that carrier mobility in columnar materials such as these are anticipated to be highly anisotropic; however, as demonstrated by the POM textures (*vide supra*), films of these materials cooled from the melt contain a mixture of differently aligned domains, with the precise mixture of alignments perhaps varying between samples and, potentially, with the effect of domain boundaries upon the mobility varying between samples. Thus, it is unlikely that our values approach the maximum 1D mobility, μ_{1D}, along the columnar stacking direction (*i.e.*, the LC director) and it is also possible that the trends we observe do not reflect those for μ_{1D}. Secondly, the transition temperatures observed on heating and cooling for **2b** bracket room temperature and, accordingly, it is unclear whether **2b** is actually in the LC phase under the measurement conditions, although POM and XRD data indicate that it certainly retains columnar order. In any case, several previous studies have shown that mobility can be highly temperature dependent in the vicinity of crystal–LC phase transitions.[16,17] Given these caveats, it is worth noting a number of trends. The compounds containing [tri(*n*-dodecyloxy)phenyl]-based mesogens (**1a–c**, **2a,b**) all show considerably higher mobility than compound **3**. Perhaps the presence of long branched alkyl substituent of **3** introduces additional disorder into the mesophase, although XRD does not show any clear evidence for different degrees of order between **1a** (the least ordered [tri(*n*-dodecyphenyl]-based species) and **3**. However, the increased mobility in **1b** and **1c** *vs.* **1a** may be related to the increased order evident in their XRD pattern. Similarly, **2b**, which XRD suggests is the most ordered of any of the species examined, shows the highest mobility. However, it also worth noting that more facile electron injection into **2b**, due to the inductive electron-withdrawing effects of the fluoroalkyl groups, may also play a role in the higher measured effective mobility.

It is worth pointing out that we encountered some variation in electrical behaviour between different devices for a given compound in the SCLC studies, with current densities varying from those corresponding to the data summarised in Table 2 to essentially immeasurable using our apparatus. Presumably this variation is related to whether or not a suitable conduction pathway of a correctly aligned domain is present between the electrodes in a given device. Several previous reports have also indicated that the ordering, alignment, and electrical behaviour of columnar materials can be strongly dependent on processing conditions and/or device geometries.[18,39,63,71] These issues represent an obstacle to exploiting these materials for organic electronic applications. Indeed, to date we have been unsuccessful in our attempts to fabricate field-effect transistors based on these materials, for which the columns must be oriented parallel to the gate dielectric surface along the source–drain axis to provide charge-transport pathways. Of possible significance is the recent report that the coronene diimide **IIb** tends to self-assemble "face down" on surfaces with the columns improperly aligned for transistor applications.[39] On the other hand, while this type of orientation might suggest the possibility of use in solar cell applications, these will require the coronene diimides to be used in combination with a hole-transport material, which raises additional questions regarding the stability of the columnar mesophases in the presence of this material and the nature of the organic–organic interface in these blends.[72]

Conclusion

Introduction of tris(3,4,5-*n*-dodecyphenyl)-based groups into either N,N' or 5,11 positions of coronene diimides has proven a successful strategy for lowering the temperature window of stability for coronene diimide columnar discotic mesophases. The use of a long-chain "swallow-tail" substituent in the N,N' positions also leads to similar transition temperatures. We have found that very high charge-carrier mobility—as high as 6.7 cm^2 V^{-1} s^{-1}—can be achieved in the columnar structures formed by these coronene diimides under ambient conditions. These mobility values represent *lower* limits for the values of the mobility in these materials due to assumptions (trap-free transport and ohmic contact) used in the determination; moreover, the 1D mobility along the columnar stacking direction is likely to be higher still. However, significant challenges remain to be overcome before these high carrier mobility values can be exploited in device applications.

Experimental details

General

All chemicals, unless otherwise noted, were purchased from Aldrich, Acros Organics, Alfa Aesar or Lancaster and were used without further purification. The ^{1}H and ^{13}C NMR spectra were acquired on Varian 300 MHz or Bruker 500 MHz spectrometers using tetramethylsilane (TMS; $\delta = 0$ ppm) as an internal standard. EI and FAB mass spectra were obtained on a VG 70SE spectrometer and MALDI mass spectra were obtained on an Applied Biosystems 4700 Proteomics Analyzer. Flash column chromatography was performed on silica gel (32–63 μm, 60 Å, Sorbent Technologies). Elemental analyses were carried out by Atlantic Microlabs using a LECO 932 CHNS elemental analyzer. DSC traces were taken on a Mettler Toledo DSC 822e instrument at 10 °C min^{-1}. XRD data were collected on a Scintag X1 diffractometer with a Cu Kα source ($\lambda = 1.5406$ Å) in a continuous scan mode with a step size of 0.02°. Optical textures were obtained using an Olympus BX51 microscope equipped with an Olympus U-TU1 X digital camera and an Instec STC200 hot stage.

3,4,5-Tri(*n*-dodecyloxy)benzonitrile.[73] A solution of BBr_3 (9.3 mL, 98.34 mmol) in dichloromethane (10 mL) was added dropwise to a solution of 3,4,5-trimethoxybenzonitrile (4.88 g, 25.25 mmol) in 30 mL dry dichloromethane at −78 °C under nitrogen. The reaction mixture was allowed to warm to room temperature and stirred for 12 h. The reaction mixture was recooled to −78 °C and ice-cold water was added dropwise. The mixture was stirred at room temperature for 2 h and then extracted with ethyl acetate; the organic solution was dried over anhydrous $MgSO_4$, filtered, and evaporated under reduced pressure to give a pale yellow solid. K_2CO_3 (13.2 g, 95.51 mmol) and 1-bromododecane (22.15 g, 88.89 mmol) were added to a solution of this solid in DMF (100 mL); the reaction mixture was then heated to 100 °C and stirred at that temperature for 42 h. After cooling to room temperature, water was added and the mixture was extracted with dichloromethane. The organic extracts were dried over $MgSO_4$, filtered, and evaporated under reduced pressure to give solids which were recrystallised from acetone to give a white solid (13.84 g, 84%). ^{1}H NMR (500 MHz, $CDCl_3$): δ 6.79 (s, 2H), 3.98 (t, $J = 6.5$ Hz, 2H), 3.94 (t, $J = 6.5$ Hz, 4H), 1.78 (m, 4H), 1.71 (m, 2H), 1.44 (m, 6H), 1.27 (m, 48H), 0.86 (t, $J = 7.0$ Hz, 9H). ^{13}C{^{1}H} NMR (125 MHz, $CDCl_3$): δ 153.4, 142.5, 119.3, 110.4, 106.1, 73.7, 69.4, 31.9, 30.3, 29.73, 29.70, 29.68, 29.65, 29.60, 29.52, 29.38, 29.35, 29.33, 29.2, 26.0, 22.7, 14.1. HRMS (EI) calcd for $C_{43}H_{77}NO_3$ (M$^+$): 655.5904. Found: 655.5925. Anal. Calcd for $C_{43}H_{77}NO_3$: C, 78.72; H, 11.83; N, 2.13. Found: C, 78.90; H, 11.96; N, 2.18.

Compound 5.[44] A solution of 3,4,5-tri(*n*-dodecyloxy)benzonitrile (12.43 g, 18.95 mmol) in dry THF (200 mL) was added to a suspension of $LiAlH_4$ (1.57 g, 42.37 mmol) in dry THF (100 mL) at 0 °C. The reaction mixture was allowed to warm to room temperature and then heated to reflux for 2 h. The reaction mixture was then cooled again at 0 °C and ice-cold water (40 mL) and then 20% aqueous NaOH (40 mL) were added dropwise. The mixture was extracted with ethyl acetate; the organic extracts were washed with brine, dried over $MgSO_4$, filtered, and evaporated under reduced pressure to give a solid which was recrystallised from acetone to give a white solid (11.23 g, 90%). ^{1}H NMR (500 MHz, C_6D_6): δ 7.08 (s, 2H), 4.21 (t, 2H), 3.67 (t, 4H), 1.87 (m, 2H), 1.63 (m, 6H), 1.37 (m, 56H), 0.92 (t, 9H). ^{13}C{^{1}H} NMR (125 MHz, C_6D_6): δ 190.4, 154.1, 144.4, 132.3, 108.1, 73.6, 69.1, 32.33, 32.32, 30.96, 30.22, 30.20, 30.19, 30.15, 30.12, 30.08, 30.02, 29.83, 29.82, 29.79, 29.66, 26.6, 26.5, 23.1, 14.3. HRMS (EI) calcd for $C_{43}H_{81}NO_3$ (M$^+$): 659.6216. Found: 659.6209.

Compound 6. Compound **4**[43] (1.07 g, 1.95 mmol) was sonicated in ^{n}BuOH–H_2O (160 mL, 1 : 1 v/v) for 10 min. **5** (3.86 g, 5.85 mmol) was added and the reaction mixture was stirred at 80 °C for 24 h. Concentrated HCl (15 mL) was added; the resultant precipitate was filtered and was purified by column chromatography eluting with chloroform–hexane (1 : 1) to give a red solid (3.01 g, 84%). ^{1}H NMR (500 MHz, $CDCl_3$): δ 9.43 (d, $J = 8.0$ Hz, 2H), 8.90 (s, 2H), 8.67 (d, $J = 8.5$ Hz, 2H), 6.79 (s, 4H), 5.26 (s, 4H), 3.94 (t, $J = 7.0$ Hz, 8H), 3.87 (t, $J = 7.0$ Hz, 4H), 1.75 (m, 8H), 1.68 (m, 4H), 1.5–1.1 (m, 108H), 0.85 (t, $J = 7.0$ Hz, 18H). ^{13}C{^{1}H} NMR (125 MHz, $CDCl_3$): δ 162.8, 163.4, 153.0, 138.2, 137.9, 132.1, 131.7, 130.2, 129.2, 128.5, 126.9, 123.2, 122.7, 120.8, 108.2, 73.4, 69.2, 44.0, 31.9, 30.3, 29.7, 29.6, 29.5, 29.4, 29.36, 26.1, 22.7, 14.1 (10 carbon resonances were not observed presumably due to near equivalencies leading to overlap of resonances). HRMS (MALDI) calcd for $C_{110}H_{165}N_2O_{10}Br_2$ (MH$^+$): 1832.0831. Found: 1832.0824. Anal. Calcd for $C_{110}H_{164}N_2O_{10}Br_2$: C, 72.03; H, 9.01; N, 1.53. Found: C, 72.23; H, 9.30; N, 1.56.

Compound 8a. $Pd(PPh_3)_4$ (0.064 g, 0.055 mmol), CuI (0.012 g, 0.063 mmol), and **7a** (0.4 mL, 2.20 mmol) were added successively to a deoxygenated suspension of **6** (1.02 g, 0.56 mmol) in toluene (35 mL) and triethylamine (3.5 mL). After the reaction mixture was heated at 65 °C under nitrogen for 22 h, it was poured into 2 N HCl solution. The solvent was removed under reduced pressure and the residue was purified by column chromatography, eluting with chloroform–hexane (2 : 1), to give a red solid (0.94 g, 87%). ^{1}H NMR (500 MHz, $CDCl_3$): δ 10.05 (d, $J = 8.5$ Hz, 2H), 8.72 (s, 2H), 8.59 (d, $J = 8.5$ Hz, 2H), 6.79 (s, 4H), 5.27 (s, 4H), 3.95 (t, $J = 6.5$ Hz, 8H), 3.87 (t, $J = 6.5$ Hz, 4H), 2.62 (t, $J = 7.0$ Hz, 4H), 1.8–1.6 (m, 16H), 1.53 (m, 4H), 1.5–1.1 (m, 124H), 0.85 (m, 24H). ^{13}C{^{1}H} NMR (125 MHz, $CDCl_3$): δ 163.3, 163.1, 153.0, 138.2, 137.8, 134.3, 133.9, 132.0, 130.4, 127.5, 127.2, 127.0, 122.8, 121.8, 121.0, 108.1, 101.5, 82.2, 73.4, 69.1, 43.9, 31.9, 31.8, 30.3, 29.73, 29.70, 29.65, 29.61, 29.46, 29.44, 29.36, 29.23, 29.21, 29.13, 28.3, 26.1, 22.7, 22.6, 20.3, 14.1 (11 carbon resonances were not observed presumably due to near equivalencies leading to overlap of resonances). HRMS (MALDI) calcd for $C_{130}H_{198}N_2O_{10}$ (M$^+$): 1947.5038. Found: 1947.5046. Anal. Calcd for $C_{130}H_{198}N_2O_{10}$: C, 80.11; H, 10.24; N, 1.44. Found: C, 80.25; H, 10.26; N, 1.46.

Compound 1a. Compound **1a** was obtained in a one-pot process from **6** and **7a** without isolation of **8a** (although **8a** was obtained pure in a separate experiment, *vide supra*). $Pd(PPh_3)_4$ (0.12 g, 0.1 mmol) and CuI (0.02 g, 0.1 mmol) were added to a deoxygenated suspension of **6** (1.47 g, 0.8 mmol) in toluene (50 mL) and triethylamine (5 mL). After further deoxygenation, **7a** (0.6 mL, 3.3 mmol) was added and the reaction mixture was heated at 65 °C under nitrogen for 24 h. DBU (0.5 mL) was added to the crude reaction mixture containing **8a**; the temperature was raised to 110 °C and the reaction mixture was stirred at this temperature under nitrogen for 21 h. After cooling to room temperature, the reaction mixture was poured into 2 N HCl solution and was extracted with dichloromethane. The organic extracts were dried over anhydrous $MgSO_4$, filtered, evaporated under reduced pressure, and purified by column chromatography eluting with chloroform–hexane (2 : 1). After repeated chromatography, a yellow solid (0.75 g, 48%) was obtained. ^{1}H NMR (500 MHz, CD_2Cl_2): δ 9.16 (s, 2H), 8.85 (s, 2H), 7.89 (s, 2H), 7.02 (s, 4H), 5.55 (s, 4H), 4.08 (br. s, 8H), 3.87 (t, $J = 6.5$ Hz, 4H), 3.36 (br. s, 4H), 2.0–1.0 (m, 144H), 0.93 (t, 6H), 0.81 (m, 18H). HRMS (MALDI) calcd for $C_{130}H_{198}N_2O_{10}$ (M^+): 1947.5046. Found: 1947.5047. Anal. Calcd for $C_{130}H_{198}N_2O_{10}$: C, 80.11; H, 10.24; N, 1.44. Found: C, 80.23; H, 10.24; N, 1.49.

Compound 8b. $Pd(PPh_3)_4$ (0.12 g, 0.10 mmol), CuI (0.02 g, 0.10 mmol), and **7b** (0.76 mL, 3.48 mmol) were added successively to a deoxygenated suspension of **6** (1.60 g, 0.87 mmol) in triethylamine (8 mL) and toluene (60 mL). After the reaction mixture was heated at 70 °C under argon for 24 h, it was cooled to room temperature and washed twice with 2 N HCl. The solvent was removed under reduced pressure and the residue was purified by column chromatography eluting with chloroform–hexane (2 : 1) to give a dark red solid (1.16 g, 73%). ^{1}H NMR (500 MHz, $CDCl_3$): δ 9.98 (d, $J = 8.0$ Hz, 2H), 8.67 (s, 2H), 8.53 (d, $J = 8.0$ Hz, 2H), 6.79 (s, 4H), 5.25 (s, 4H), 3.95 (t, $J = 6.5$ Hz, 8H), 3.86 (t, $J = 6.5$ Hz, 4H), 2.61 (t, $J = 2.61$ Hz, 4H), 1.8–1.6 (m, 16H), 1.6–1.1 (m, 136H), 0.86 (m, 24H). ^{13}C{^{1}H} NMR (125 MHz, $CDCl_3$): δ 163.2, 163.0, 153.0, 138.2, 137.8, 134.1, 133.7, 132.0, 130.3, 127.4, 127.2, 126.8, 122.7, 121.7, 120.9, 108.0, 101.7, 82.2, 73.4, 69.1, 43.9, 31.9, 30.3, 29.73, 29.72, 29.71, 29.67, 29.65, 29.61, 29.56, 29.47, 29.45, 29.4, 29.3, 29.26, 29.19, 28.3, 26.1, 22.7, 20.3, 14.1 (12 carbon resonances were not observed presumably due to near equivalencies leading to overlap of resonances). Anal. Calcd for $C_{134}H_{206}N_2O_{10}$: C, 80.27; H, 10.36; N, 1.40. Found: C, 80.28; H, 10.39; N, 1.45.

Compound 1b. A solution of DBU (0.32 mL) and **8b** (1.09 g, 0.54 mmol) in toluene (100 mL) was heated to 100 °C under argon. After 20 h, the mixture was allowed to cool to room temperature and washed twice with 2 N HCl. The solvent was removed under reduced pressure and the residue was purified by column chromatography, eluting with dichloromethane, to give a yellow solid (0.90 g, 83%). ^{1}H NMR (500 MHz, $CDCl_3$): δ 9.56 (s, 2H), 9.29 (s, 2H), 8.28 (s, 2H), 7.05 (s, 4H), 5.62 (s, 4H), 4.08 (br. s, 8H), 3.88 (t, $J = 7.0$ Hz, 4H), 3.58 (br. s, 4H), 1.98 (m, 4H), 1.78 (m, 8H), 1.68 (m, 4H), 1.59 (m, 4H), 1.5–1.1 (m, 136H), 0.85 (m, 24H). ^{13}C NMR (125 MHz, $CDCl_3$): δ 163.8, 163.6, 153.2, 140.2, 138.0, 132.3, 128.7, 127.6, 127.0, 126.6, 124.8, 120.8, 120.4, 120.1, 119.8, 119.5, 118.1, 108.5, 73.3, 69.2, 44.26, 33.4, 32.0, 31.9, 30.8, 30.4, 30.0, 29.8, 29.71, 29.68, 29.64, 29.61, 29.53, 29.45, 29.4, 29.3, 26.2, 26.1, 22.7, 22.6, 14.1, 14.0 (11 carbon resonances were not observed presumably due to near equivalencies leading to overlap of resonances). HRMS (MALDI) calcd for $C_{134}H_{207}N_2O_{10}$ (MH^+): 2004.5751. Found: 2004.5746. Anal. Calcd for $C_{134}H_{206}N_2O_{10}$: C, 80.27; H, 10.36; N, 1.40. Found: C, 80.26; H, 10.35; N, 1.45.

Compound 8c. $Pd(PPh_3)_4$ (0.12 g, 0.1 mmol), CuI (0.02 g, 0.1 mmol), and **7c** (1.2 mL, 4.3 mmol) were added successively to a deoxygenated suspension of compound **6** (2.0 g, 1.1 mmol) in toluene (70 mL) and triethylamine (10 mL). The resulting solution was further deoxygenated and heated to 70 °C under nitrogen for 42 h. After cooling, the mixture was poured into 2 N HCl solution. The solvent was removed and the residue was purified by column chromatography eluting with chloroform–hexane (2 : 1) to give a red solid (1.96 g, 85%). ^{1}H NMR (500 MHz, $CDCl_3$): δ 9.95 (d, $J = 8.5$ Hz, 2H), 8.57 (s, 2H), 8.49 (d, $J = 8.0$ Hz, 2H), 6.79 (s, 4H), 5.28 (s, 4H), 3.95 (t, $J = 6.0$ Hz, 8H), 3.86 (t, $J = 6.5$ Hz, 4H), 2.61 (t, $J = 7.0$ Hz, 4H), 1.8–1.6 (m, 16H), 1.6–1.1 (m, 152H), 0.85 (t, $J = 7.0$ Hz, 24H). ^{13}C{^{1}H} NMR (125 MHz, $CDCl_3$): δ 163.1, 162.9, 153.0, 138.1, 137.8, 134.0, 133.6, 131.9, 130.2, 127.3, 127.1, 126.8, 122.7, 121.7, 120.9, 108.0, 101.8, 82.2, 73.3, 69.1, 43.9, 31.9, 30.3, 29.71, 29.65, 29.57, 29.47, 29.45, 29.36, 29.3, 29.2, 28.3, 26.1, 22.7, 20.3, 14.1 (21 carbon resonances were not observed presumably due to near equivalencies leading to overlap of resonances). MS (MALDI): *m/z* 2116.8 (MH^+). Anal. Calcd for $C_{142}H_{222}N_2O_{10}$: C, 80.55; H, 10.57; N 1.32. Found: C, 80.69; H, 10.68; N, 1.36.

Compound 1c. A solution of **8c** (1.78 g, 0.84 mmol) and DBU (1 mL) in toluene (50 mL) was heated at 110 °C under argon for 42 h. After cooling, the reaction mixture was poured into 2 N HCl and extracted with hexane. After removal of solvent under reduced pressure, the material was purified by column chromatography eluting with chloroform–hexane (1 : 1) to give a yellow solid (0.65 g, 37%). ^{1}H NMR (500 MHz, $CDCl_3$): δ 9.55 (s, 2H), 9.27 (s, 2H), 8.26 (s, 2H), 7.05 (s, 4H), 5.62 (s, 4H), 4.08 (br. s, 8H), 3.89 (t, $J = 6.5$ Hz, 4H), 3.57 (br. s, 4H), 1.97 (br. m, 4H), 1.78 (m, 8H), 1.69 (m, 4H), 1.65 (m, 4H), 1.5–1.1 (m, 148H), 0.84 (m, 24H). ^{13}C{^{1}H} NMR (125 MHz, $CDCl_3$): δ 164.1, 163.9, 153.2, 140.7, 138.0, 132.4, 129.1, 128.1, 127.5, 127.1, 125.2, 121.4, 120.9, 120.7, 120.4, 120.2, 118.8, 108.4, 73.4, 69.3, 44.4, 33.6, 31.93, 31.88, 31.1, 30.4, 29.96, 29.79, 29.78, 29.76, 29.70, 29.68, 29.64, 29.63, 29.57, 29.53, 29.4, 29.3, 26.2, 26.1, 22.7, 22.6, 14.09, 14.06 (13 carbon resonances were not observed presumably due to near equivalencies leading to overlap of resonances). HRMS (MALDI) calcd for $C_{142}H_{222}N_2O_{10}$ (M^+): 2115.6924. Found: 2115.6920. Anal. Calcd for $C_{142}H_{222}N_2O_{10}$: C, 80.55; H, 10.57; N, 1.32. Found: C, 80.32; H, 10.50; N, 1.35.

Compound 10b. Compound **4** (0.93 g, 1.68 mmol) was sonicated in NMP (20 mL) for 30 min, and acetic acid (0.645 g, 11.80 mmol) followed by a solution of **9b** (2.0 g, 4.86 mmol) in NMP (15 mL) were added. After the reaction mixture was heated at 85 °C under nitrogen for 8 h, it was allowed to cool to room temperature. Methanol (150 mL) was added, the resulting precipitate was collected by filtration and purified by column chromatography, eluting with chloroform, to give a red solid (1.25 g, 57%). ^{1}H NMR (500 MHz, $CDCl_3$): δ 9.51 (d, $J = 8.0$ Hz, 2H), 8.97 (s, 2H), 8.75 (d, $J = 8.0$ Hz, 2H), 5.03 (m, 4H). HRMS (MALDI) calcd for $C_{40}H_{10}N_2O_4F_{30}Br_2$ (M^+): 1309.8528. Found:

1309.8528. Anal. Calcd for $C_{40}H_{10}Br_2F_{30}N_2O_4$: C, 36.61; H, 0.77; N, 2.13. Found: C, 36.68; H, 0.66; N, 2.07.

Compound 11. 4-Dimethylpyridine (0.44 g, 3.59 mmol) was added to a solution of 3,4,5-tris(*n*-dodecyloxy)benzoyl chloride[74,75] (1.56 g, 2.25 mmol). Pent-4-yn-1-ol (0.26 g, 3.10 mmol) was added *via* a syringe under nitrogen and the reaction mixture was stirred for 80 min at room temperature. The solvent was then removed under reduced pressure; the residue was purified by column chromatography eluting with ethyl acetate–hexane (1 : 19) to give a white solid (1.37 g, 82%). ^1H NMR (300 MHz, $CDCl_3$): δ 7.23 (s, 2H), 4.38 (t, $J = 6.3$ Hz, 2H), 3.98 (m, 6H), 2.34 (dt, $J = 7.2, 2.4$ Hz, 2H), 1.97 (m, 3H), 1.86–1.68 (m, 6H), 1.54–1.16 (m, 59H), 0.86 (m, 9H). $^{13}C\{^1H\}$ NMR (75 MHz, $CDCl_3$): δ 166.2, 152.7, 142.3, 124.6, 108.0, 83.0, 73.5, 69.2, 69.0, 63.5, 32.0, 30.4, 29.8, 29.73, 29.70, 29.6, 29.5, 29.4, 27.8, 26.2, 26.1, 22.8, 15.5, 14.2 (10 carbon resonances were not observed presumably due to near equivalencies leading to overlap of resonances). HRMS (MALDI) calcd for $C_{48}H_{85}O_5$ (MH^+): 741.6397. Found: 741.6392. Anal. Calcd for $C_{48}H_{84}O_5$: C, 77.78; H, 11.42. Found: C, 77.54; H, 11.47.

Compound 12a. $Pd(PPh_3)_4$ (0.06 g, 0.05 mmol) and CuI (0.015 g, 0.17 mmol) were added to a deoxygenated solution of **10a**[34] (0.42 g, 0.54 mmol) in toluene (30 mL) and triethylamine (6 mL). A deoxygenated solution of **11** (1.20 g, 1.62 mmol) in toluene (10 mL) was then added; the reaction mixture was heated to 60 °C under nitrogen for 14 h, after which it was allowed to cool to room temperature and poured into 2 N HCl solution. The organic phase was separated and was washed with water. The solvent was removed under reduced pressure and the residue was purified by column chromatography, eluting with dichloromethane, to give a red solid (1.01 g, 89%). ^1H NMR (500 MHz, $CDCl_3$): δ 10.07 (d, $J = 8.5$ Hz, 2H), 8.65 (s, 2H), 8.61 (d, $J = 8.0$ Hz, 2H), 7.21 (s, 4H), 4.55 (t, $J = 6.0$ Hz, 4H), 4.16 (t, $J = 8.0$ Hz, 4H), 3.88 (t, $J = 6.5$ Hz, 8H), 3.82 (t, $J = 6.5$ Hz, 4H), 2.86 (t, $J = 6.5$ Hz, 4H), 2.25 (m, 4H), 1.8–1.6 (m, 16H), 1.5–1.1 (m, 128H), 0.87 (m, 24H). Anal. Calcd for $C_{136}H_{206}N_2O_{14}$: C, 78.04; H, 9.92; N, 1.34. Found: C, 77.82; H, 9.97; N, 1.50.

Compound 2a. DBU (0.2 mL) was added *via* syringe to a solution of **12a** (0.72 g, 0.34 mmol) in toluene (50 mL), and the resulting solution was heated to 100 °C under nitrogen for 20 h. After cooling to room temperature, the reaction mixture was poured into 2 N HCl solution. The organic layer was separated, and the solvent was removed under reduced pressure. The residue was purified by column chromatography, eluting first with dichloromethane and then with 5% ethyl acetate–dichloromethane (1 : 19), to give a yellow solid (0.58 g, 80%). ^1H NMR (500 MHz, CD_2Cl_2): δ 9.61 (s, 2H), 9.34 (s, 2H), 8.60 (s, 2H), 6.89 (s, 4H), 4.60 (t, $J = 6.0$ Hz, 4H), 4.44 (t, $J = 8.0$ Hz, 4H), 3.87 (t, $J = 6.0$ Hz, 4H), 3.64 (m, 12H), 2.62 (m, 4H), 1.94 (m, 4H), 1.7–1.1 (m, 140H), 1.0–0.7 (m, 24H). HRMS (MALDI) calcd for $C_{136}H_{207}N_2O_{14}$ (MH^+): 2092.5547. Found: 2092.5543. Anal. Calcd for $C_{136}H_{206}N_2O_{14}$: C, 78.04; H, 9.92; N, 1.34. Found: C, 77.85; H, 9.88; N, 1.47.

Compound 2b. $Pd(PPh_3)_4$ (0.075 g, 0.065 mmol), CuI (0.023 g, 0.12 mmol), and **11** (1.31 g, 1.77 mmol) were added successively to a deoxygenated suspension of compound **10b** (0.77 g, 0.59 mmol) in toluene (40 mL) and triethylamine (10 mL). The reaction mixture was heated at 65 °C for 18 h. After cooling to room temperature, the reaction mixture was poured into 2 N HCl solution. The organic layer was separated and the solvent was removed under reduced pressure. The residue was purified by column chromatography, eluting with dichloromethane–chloroform, to afford a mixture of red and yellow compounds, presumably **12b** and **2b**, respectively. This crude mixture was then dissolved in toluene (90 mL) and was heated to 100 °C under nitrogen; DBU (0.35 mL) was added and the reaction was maintained at 100 °C for 19 h under nitrogen. After cooling to room temperature, the reaction mixture was poured into 2 N HCl solution. The organic layer was separated and the solvent was removed under reduced pressure. The residue was purified by column chromatography eluting with chloroform, 0.62 g (37%) of a yellow–brown solid was obtained. ^1H NMR (500 MHz, $CDCl_3$): δ 9.89 (s, 2H), 9.64 (s, 2H), 8.84 (s, 2H), 6.89 (s, 4H), 5.31 (t, $J = 15.7$ Hz, 4H), 4.60 (t, $J = 6.0$ Hz, 4H), 3.94 (m, 4H), 3.75 (t, $J = 6.5$ Hz, 4H), 3.69 (t, $J = 6.5$ Hz, 8H), 2.66 (m, 4H), 1.8–1.55 (m, 12H), 1.5–1.1 (m, 108H), 0.83 (m, 18H). Anal. Calcd for $C_{136}H_{176}F_{30}N_2O_{14}$: C, 62.04; H, 6.74; N, 1.06. Found: C, 61.98; H, 6.69; N, 1.10.

Compound 14. Compound **14** was synthesised from **4** and **13**[45] as described previously.[76]

Compound 3. Compound **3** was obtained in a one-pot process from **14** and **7a** without isolation of **15**. $Pd(PPh_3)_4$ (0.28 g, 0.24 mmol), CuI (0.034 g, 0.18 mmol), and **7a** (1.3 mL, 7.20 mmol) were added successively to a deoxygenated solution of **14** (2.2 g, 1.8 mmol) in toluene (50 mL) and triethylamine (10 mL). The reaction mixture was heated at 65 °C under nitrogen for 24 h. DBU (0.5 mL) was added and the reaction temperature was raised to 100 °C and stirred for another 16 h. Additional DBU (0.5 mL) was added and the reaction temperature was raised to 110 °C and the reaction mixture was further stirred at this temperature for 24 h. The reaction mixture was cooled to room temperature, poured into 2 N HCl solution, and extracted with dichloromethane. The organic extracts were evaporated under reduced pressure and the residue was purified by column chromatography, eluting with chloroform–hexane (1 : 3) to give a yellow solid (1.9 g, 86%). ^1H NMR (500 MHz, $CDCl_3$): δ 9.32 (s, 2H), 9.10 (s, 2H), 8.25 (s, 2H), 4.42 (d, $J = 7.0$ Hz, 4H), 3.52 (t, $J = 7.0$ Hz, 4H), 2.15 (m, 2H), 2.00 (m, 4H), 1.63 (m, 4H), 1.55–1.0 (m, 104H), 0.91 (t, $J = 7.0$ Hz, 6H), 0.80 (m, 12H). $^{13}C\{^1H\}$ NMR (125 MHz, $CDCl_3$): δ 164.9, 164.7, 141.1, 129.4, 128.7, 128.1, 127.5, 125.5, 122.1, 121.5, 121.0, 120.8, 120.7, 119.5, 45.5, 37.5, 34.0, 32.4, 32.3, 31.3, 30.64, 30.62, 30.4, 30.1, 30.07, 30.01, 29.9, 29.74, 29.70, 27.1, 23.2, 23.0, 14.6, 14.5 (11 carbon resonances were not observed presumably due to near equivalencies leading to overlap of resonances). HRMS (MALDI) calcd for $C_{90}{}^{13}C_2H_{138}N_2O_4$ (M^+): 1337.0724. Found: 1337.0807. Anal. Calcd for $C_{92}H_{138}N_2O_4$: C, 82.70; H, 10.41; N, 2.10. Found: C, 82.82; H, 10.55; N, 2.21.

Sample preparation and mobility measurements

The ITO-covered glass substrates were cleaned using ultrasonic treatment in detergent water, water, DI water, acetone, ethanol, and dried at 60 °C in a vacuum oven overnight, and finally treated with high-pressure N_2 gas flow. Prior to the fabrication of the device, ITO-covered glass substrates were plasma treated (750 W) for 5 min. A small amount of the coronene diimide compound was melted at a temperature above its isotropic clearing point on an ITO-coated glass substrate on a digital hot plate in air. Compounds **1a–c** were melted at 210 °C, compounds **2a** and **2b** at 220 °C and 210 °C, respectively, and compound **3** was processed at 285 °C. While kept in the isotropic phase on the first ITO substrate, the compounds were sandwiched using a silver-coated glass substrate to form a device. Calibrated glass spacers were used to ensure a uniform sample thickness of 5 μm. The device with the compound in the isotropic phase was removed from the hot plate and allowed to cool down in air to room temperature. During the cooling process, a slight exterior force without shear was applied in order to enhance the contact between organic layer and the electrodes. The active area of each device was in the range of 3 to 5 mm^2. Prior to the current–voltage characteristic measurement, devices were sealed with quick-setting epoxy adhesive. The silver electrodes were fabricated on glass substrates by thermal evaporation of silver using a SPECTROS Kurt J. Lesker System at a vacuum of 10^{-7} Torr through shadow masks. On each glass substrate four silver electrodes with a thickness in the range of 150 to 350 nm were formed. Prior to the silver deposition, the 1″ × 1″ glass slides were cleaned using the same procedure as the cleaning of ITO-coated glass slides. For SCLC experiments, the measurements of J–V characteristics of all devices were performed at room temperature in air and in the dark. The J–V characteristics were measured using a Keithley 2400 Source Meter. Capacitance was measured using Agilent 16048A Test Leads connected to an Agilent 4284A Precision LCR Meter.

Acknowledgements

This material is based upon work supported in part by the STC Program of the National Science Foundation under Agreement Number DMR-0120967. We also thank the NSF for funding through CHE-0211419.

References

1 S. Laschat, A. Baro, N. Steinke, F. Giesselmann, C. Hägele, G. Scalia, R. Judele, E. Kapatsina, S. Sauer, A. Schreivogel and M. Tosoni, *Angew. Chem., Int. Ed.*, 2007, **46**, 4832.

2 In some other examples of columnar discotic mesophases the redox activity is associated with electroactive moieties located in arms surrounding the core, rather than with the core itself, the arms being either conjugated to the core (for example: Y.-D. Zhang, K. G. Jespersen, M. Kempe, J. A. Kornfield, S. Barlow, B. Kippelen and S. R. Marder, *Langmuir*, 2003, **19**, 6534) or linked through saturated bridging groups to the core (for example: I. Paraschiv, K. de Lange, M. Giesbers, B. van Lagen, F. C. Grozema, R. D. Abellon, L. D. A. Siebbeles, E. J. R. Sudhölter, H. Zuilhof and A. T. M. Marcelis, *J. Mater. Chem.*, 2008, **18**, 5475).

3 I. Seguy, P. Destruel and H. Bock, *Synth. Met.*, 2000, **111–112**, 15.

4 L. Schmidt-Mende, A. Fechtenkötter, K. Müllen, E. Moons, R. H. Friend and J. D. MacKenzie, *Science*, 2001, **293**, 1119.

5 M. Lehmann, G. Kestemont, R. G. Aspe, C. Buess-Herman, M. H. J. Koch, M. G. Debije, J. Piris, M. P. de Haas, J. M. Warman, M. D. Watson, V. Lemaur, J. Cornil, Y. H. Geerts, R. Gearba and D. A. Ivanov, *Chem.–Eur. J.*, 2005, **11**, 3349.

6 H. Iino, J.-i. Hanna, R. J. Bushby, B. Movaghar, B. J. Whitaker and M. J. Cook, *Appl. Phys. Lett.*, 2005, **87**, 132102.

7 H. Iino, Y. Takayashiki, J.-i. Hannaa, R. J. Bushby and D. Haarer, *Appl. Phys. Lett.*, 2005, **87**, 192105.

8 Q. Zhang, P. Prins, S. C. Jones, S. Barlow, T. Kondo, L. D. A. Siebbeles and S. R. Marder, *Org. Lett.*, 2005, **7**, 5019.

9 M. Kastler, W. Pisula, F. Laquai, A. Kumar, R. J. Davies, S. Baluschev, M.-C. Garcia-Gutiérrez, D. Wasserfallen, H.-J. Butt, C. Riekel, G. Wegner and K. Müllen, *Adv. Mater.*, 2006, **18**, 2255.

10 V. Duzhko, A. Semyonov, R. J. Twieg and K. D. Singer, *Phys. Rev. B: Condens. Matter*, 2006, **73**, 064201.

11 W. Pisula, M. Kastler, D. Wasserfallen, M. Mondeshki, J. Piris, I. Schnell and K. Müllen, *Chem. Mater.*, 2006, **18**, 3634.

12 B. R. Kaafarani, L. A. Lucas, B. Wex and G. E. Jabbour, *Tetrahedron Lett.*, 2007, **48**, 5995.

13 Y. Hirai, H. Monobe, N. Mizoshita, M. Moriyama, K. Hanabusa, Y. Shimizu and T. Kato, *Adv. Funct. Mater.*, 2008, **18**, 1668.

14 M. Talarico, R. Termine, E. M. García-Frutos, A. Omenat, J. L. Serrano, B. Gómez-Lor and A. Golemme, *Chem. Mater.*, 2008, **20**, 6589.

15 R. Chaudhuri, M.-Y. Hsu, C.-W. Li, C.-I. Wang, C.-J. Chen, C. K. Lai, L.-Y. Chen, S.-H. Liu, C.-C. Wu and R.-S. Liu, *Org. Lett.*, 2008, **10**, 3053.

16 A. M. van de Craats, J. M. Warman, A. Fechtenkötter, J. D. Brand, M. A. Harbison and K. Müllen, *Adv. Mater.*, 1999, **11**, 1469.

17 M. G. Debije, J. Piris, M. P. de Haas, J. M. Warman, Ž. Tomović, C. D. Simpson, M. D. Watson and K. Müllen, *J. Am. Chem. Soc.*, 2004, **126**, 4641.

18 Z. An, J. Yu, S. C. Jones, S. Barlow, S. Yoo, B. Domercq, P. Prins, L. D. A. Siebbeles, B. Kippelen and S. R. Marder, *Adv. Mater.*, 2005, **17**, 2580.

19 G. Horowitz, F. Kouki, P. Spearman, D. Fichou, C. Nogues, X. Pan and F. Garnier, *Adv. Mater.*, 1996, **8**, 242.

20 C. W. Struijk, A. B. Sieval, J. E. J. Dakhorst, M. van Dijk, P. Kimkes, R. B. M. Koehorst, H. Donker, T. J. Schaafsma, S. J. Picken, A. M. van de Craats, J. M. Warman, H. Zuilhof and E. J. R. Sudholter, *J. Am. Chem. Soc.*, 2000, **122**, 11057.

21 P. R. L. Malenfant, C. D. Dimitrakopoulos, J. D. Gelorme, L. L. Kosbar and T. O. Graham, *Appl. Phys. Lett.*, 2002, **80**, 2517.

22 B. J. Jones, M. J. Ahrens, M. H. Yoon, A. Facchetti, T. J. Marks and M. R. Wasielewski, *Angew. Chem., Int. Ed.*, 2004, **43**, 6363.

23 Z. Chen, M. G. Debije, T. Debaedemaeker, P. Osswald and F. Würthner, *ChemPhysChem*, 2004, **5**, 137.

24 R. Schmidt, M. M. Ling, J. H. Oh, M. Winkler, M. Könemann, B. Zhenan and F. Würthner, *Adv. Mater.*, 2007, **19**, 3692.

25 F. Würthner, P. Osswald, R. Schmidt, T. E. Kaiser, H. mansikkamäki and M. Könemann, *Org. Lett.*, 2006, **8**, 3765.

26 B. J. Jones, A. Facchetti, M. R. Wasielewski and T. J. Marks, *J. Am. Chem. Soc.*, 2007, **129**, 15259.

27 J. H. Oh, S. Liu, Z. Bao, R. Schmidt and F. Würthner, *Appl. Phys. Lett.*, 2007, **91**, 212107.

28 H. Z. Chen, M. M. Ling, X. Mo, M. M. Shi, M. Wang and Z. Bao, *Chem. Mater.*, 2007, **19**, 816.

29 Y. Wang, Y. Chen, R. Li, S. Wang, W. Su, P. Ma, M. R. Wasielewski, X. Li and J. Jiang, *Langmuir*, 2007, **23**, 5836.

30 Y. Li, L. Tan, Z. Wang, H. Qian, Y. Shi and W. Hu, *Org. Lett.*, 2008, **10**, 529.

31 R. J. Chesterfield, J. C. McKeen, C. R. Newman, P. C. Ewbank, D. A. da Silva Filho, J.-L. Brédas, L. L. Miller, K. R. Mann and C. D. Frisbie, *J. Phys. Chem. B*, 2004, **108**, 19281.

32 A. van de Craats and J. M. Warman, *Adv. Mater.*, 2001, **13**, 130.

33 U. Rohr, P. Schlichting, A. Böhm, M. Gross, K. Meerholz, C. Bräuchle and K. Müllen, *Angew. Chem., Int. Ed.*, 1998, **37**, 1434.

34 U. Rohr, C. Kohl, K. Müllen, A. van de Craats and J. Warman, *J. Mater. Chem.*, 2001, **11**, 1789.

35 M. Adachi and Y. Nagao, *Chem. Mater.*, 2001, **13**, 662.

36 P. Samorí, N. Severin, C. D. Simpson, K. Müllen and J. P. Rabe, *J. Am. Chem. Soc.*, 2002, **124**, 9454.

37 M. Franceschin, A. Alvino, G. Ortaggi and A. Bianco, *Tetrahedron Lett.*, 2004, **45**, 9015.

38 S. Müller and K. Müllen, *Chem. Commun.*, 2005, 4045.

39 F. Nolde, W. Pisula, S. Müller, C. Kohl and K. Müllen, *Chem. Mater.*, 2006, **18**, 3715.

40 S. Alibert-Fouet, I. Seguy, J.-F. Bobo, P. Destruel and H. Bock, *Chem.–Eur. J.*, 2007, **13**, 1746.

41 Y. Avlasevich, S. Müller, P. Erk and K. Müllen, *Chem.–Eur. J.*, 2007, **13**, 6555.

42 M. Franceschin, A. Alvino, V. Casagrande, C. Mauriello, E. Pascucci, M. Savino, G. Ortaggi and A. Bianco, *Bioorg. Med. Chem.*, 2007, **15**, 1848.

43 A. Boehm, H. Arms, G. Henning and P. Blaschka, German Patent, DE 95–19547209, 1997.

44 J. van Herrikhuyzen, A. Syamakumari, A. P. H. J. Schenning and E. W. Meijer, *J. Am. Chem. Soc.*, 2004, **126**, 10026.

45 M. Conrads, A. T. Herrmann, E. Scherf and A. Wagner, European Patent 742199, 1996.

46 K. Sonogashira, Y. Tohda and N. Hagihara, *Tetrahedron Lett.*, 1975, **50**, 4467.

47 F. Würthner, V. Stepanenko, Z. Chen, C. R. Saha-Möller, N. Kocher and D. Stalke, *J. Org. Chem.*, 2004, **69**, 7933.

48 F. Würthner, C. Thalacker, S. Diele and C. Tschierske, *Chem.–Eur. J.*, 2001, **7**, 2245.

49 See discussion in ref. 18 (in footnote 12) of alternative estimates. However, the estimate of 4.1 eV for perylene diimides is broadly in line with an EA of 4.0 eV measured by inverse photoelectron spectroscopy for films of perylene-3,4:9,10-dianhydride (C. K. Chan, E.-G. Kim, J.-L. Brédas and A. Kahn, *Adv. Funct. Mater.*, 2006, **16**, 831).

50 H. E. Katz, J. Johnson, A. J. Lovinger and W. Li, *J. Am. Chem. Soc.*, 2000, **122**, 7787.

51 For example, see: C. P. Jariwal and L. J. Mathias, *Macromolecules*, 1993, **26**, 5129; Y. Yanagimoto, Y. Takaguchi, Y. Sako, S. Tsuboi, M. Ichihara and K. Ohta, *Tetrahedron*, 2006, **62**, 8373; N. Terasawa, H. Monobe and K. Kiyohara, *Liq. Cryst.*, 2007, **34**, 311.

52 A. Fechtenkötter, K. Saalwächter, M. A. Harbison, K. Müllen and H. W. Spiess, *Angew. Chem., Int. Ed.*, 1999, **38**, 3099.

53 D. Adam, P. Schuhmacher, J. Simmerer, L. Häussling, K. Siemensmeyer, K. H. Etzbach, H. Ringsdorf and D. Haarer, *Nature*, 1994, **371**, 141.

54 P. W. M. Blom, M. J. M. de Jong and M. G. van Munster, *Phys. Rev. B: Condens. Matter*, 1997, **55**, R656.

55 L. Bozano, S. A. Carter, J. C. Scott, G. G. Malliaras and P. J. Brock, *Appl. Phys. Lett.*, 1999, **74**, 1132.

56 J. Reynaert, V. I. Arkhipov, G. Borghs and P. Heremans, *Appl. Phys. Lett.*, 2004, **85**, 603.

57 P. W. M. Blom, C. Tanase, D. M. de Leeuw and R. Coehoorn, *Appl. Phys. Lett.*, 2005, **86**, 092105.

58 B. R. Kaafarani, T. Kondo, J. Yu, Q. Zhang, D. Dattilo, C. Risko, S. C. Jones, S. Barlow, B. Domercq, F. Amy, A. Khan, J. L. Brédas, B. Kippelen and S. R. Marder, *J. Am. Chem. Soc.*, 2005, **127**, 16358.

59 E. Zhou, Z. Tan, L. Huo, Y. He, C. Yang and Y. Li, *J. Phys. Chem. B*, 2006, **110**, 26062.

60 J. E. Parmer, A. C. Mayer, B. E. Hardin, S. R. Scully, M. D. McGehee, M. Heeney and I. McCulloch, *Appl. Phys. Lett.*, 2008, **92**, 113309/1.

61 C. H. Woo, B. C. Thompson, B. J. Kim, M. F. Toney and J. M. J. Fréchet, *J. Am. Chem. Soc.*, 2008, **130**, 16324.

62 M. Giulianini, E. R. Waclawik, J. M. Bell and N. Motta, *Appl. Phys. Lett.*, 2009, **94**, 083302.

63 J.-Y. Cho, J. Yu, B. Domercq, S. C. Jones, S. Barlow, B. Kippelen and S. R. Marder, *J. Mater. Chem.*, 2007, **17**, 2642.

64 B. Domercq, J. Yu, B. R. Kaafarani, T. Kondo, S. Yoo, J. N. Haddock, S. Barlow, S. R. Marder and B. Kippelen, *Mol. Cryst. Liq. Cryst.*, 2008, **481**, 80.

65 R. W. I. de Boer, M. Jochemsen, T. M. Klapwijk, A. F. Morpurgo, J. Niemax, A. K. Tripathi and J. Pflaum, *J. Appl. Phys.*, 2004, **95**, 1196.

66 W. Xu, Khizar-ul-Haq, Y. Bai, X. Y. Jiang and Z. L. Zhang, *Solid State Commun.*, 2008, **146**, 311.

67 C. H. Cheung, K. C. Kwok, S. C. Tse and S. K. So, *J. Appl. Phys.*, 2008, **103**, 093705/1.

68 G. Schwartz, T.-H. Ke, C.-C. Wu, K. Walzer and K. Leo, *Appl. Phys. Lett.*, 2008, **93**, 073304.

69 P. N. Murgatroyd, *J. Phys. D: Appl. Phys.*, 1970, **3**, 151.

70 P. M. Borsenberger, L. Pautmeier and H. Bässler, *J. Chem. Phys.*, 1991, **94**, 5447.

71 V. De Cupere, J. Tant, P. Viville, R. Lazzaroni, W. Osikowicz, W. R. Salaneck and Y. H. Geerts, *Langmuir*, 2006, **22**, 7798.

72 L. Schmidt-Mende, M. Watson, K. Müllen and R. H. Friend, *Mol. Cryst. Liq. Cryst.*, 2003, **396**, 73.

73 M. Lee, Y.-S. Yoo and M.-G. Choi, *Bull. Korean Chem. Soc.*, 1997, **18**, 1067.

74 V. Percec, D. Schlueter, J. C. Ronda, G. Johansson, G. Ungar and J. P. Zhou, *Macromolecules*, 1996, **29**, 1464.

75 D. J. P. Yeardley, G. Ungar, V. Percec, M. N. Holerca and G. Johansson, *J. Am. Chem. Soc.*, 2000, **122**, 1684.

76 X. Zhan, Z. Tan, B. Domercq, Z. An, X. Zhang, S. Barlow, Y. Li, D. Zhu, B. Kippelen and S. R. Marder, *J. Am. Chem. Soc.*, 2007, **129**, 7246.